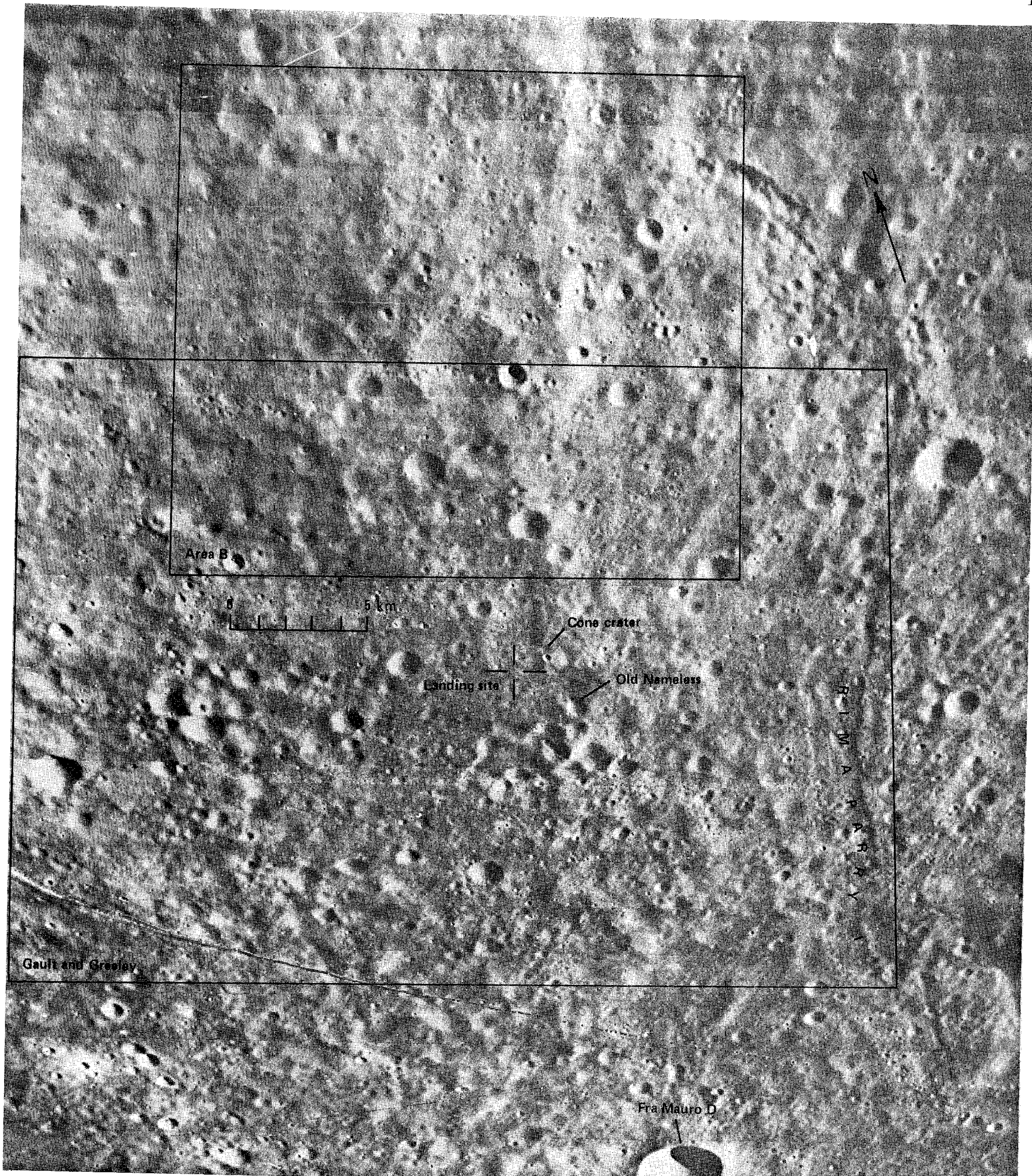

FIGURE 7.—Lunar Orbiter III, Frame 133M showing area B, which was also counted on Lunar Orbiter IV, Frame 120H3 of figure 5.

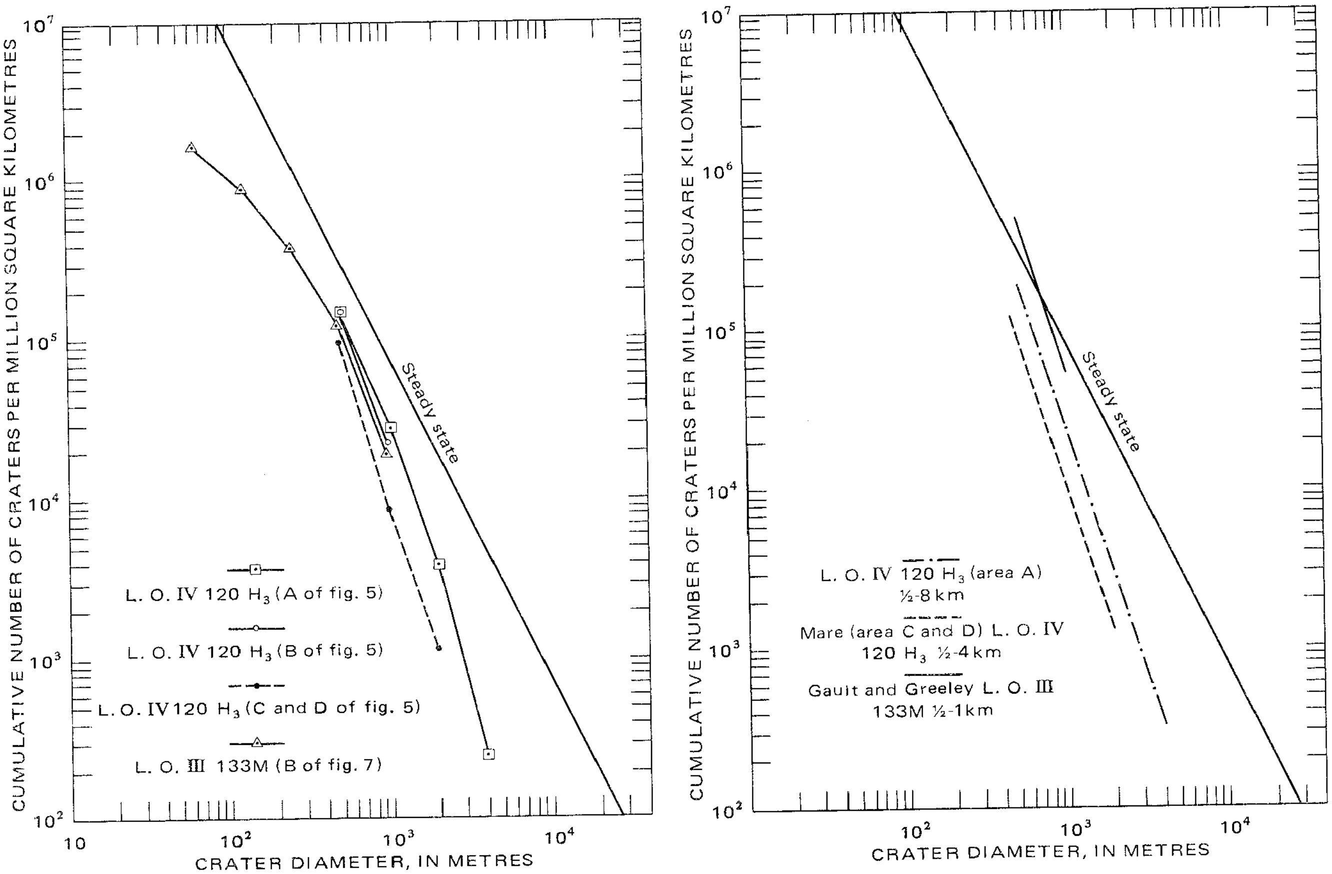

FIGURE 8.—Size frequency distribution of craters. *A*, Comparison of crater counts on the Fra Mauro Formation (areas A and B) and on the adjacent mare (areas C and D). (See figs. 5 and 7.) *B*, Comparison of production functions of craters for the Fra Mauro Formation determined from Lunar Orbiter III, Frame 133M (1,540 km^2) and from Lunar Orbiter IV, Frame 120H3 (8,172 km^2).

within the boundaries. The number of craters in each parcel is then normalized to an area of 10^6km^2. Cumulative numbers of craters are plotted on log-log coordinates (fig. 8*A*), and best-fit curves are calcualted by the least squares method for craters ½km or more in diameter. The theoretical steady-state function described by Trask (1966) is shown for comparison. Crater data are tabulated in table 1, which also gives the $\log_{10}$ cumulative numbers per 10^6km^2 and the derived crater ratio of Fra Mauro:mare.

The crater counts (fig. 8*A*) show that in the size range from ½ to 4 km, the Fra Mauro Formation has about 1.5 to 3.3 times as many craters as does the adjacent mare, which supports the inference that the Fra Mauro Formation is older. The mare in areas C and D has a crater density corresponding closely to that at the Apollo 11 site (Shoemaker and others, 1970; Gault and Greeley, oral commun., 1972).

We find only about half as many craters on the Fra Mauro Formation as do Gault and Greeley (oral commun., 1972) (fig. 8*B*), probably because of differences in crater recognition and in the sizes of the areas counted.

Craters smaller than 400 m are not as numerous on the Fra Mauro as on the adjacent mare (Trask, 1966), probably because the regolith is thicker and the slopes higher at the Fra Mauro site. Small craters in the lunar regolith are probably destroyed at a faster rate by downslope movement of loose debris on the rolling hills of the Fra Mauro area than on the more level mare surfaces (Soderblom, 1970). Also, soil at the Apollo 14 site apparently has a lower cohesion at shallow depths than that at earlier landing sites, which were on the maria (Mitchell and others, 1971).

On the basis of the diameters of the smallest craters that penetrate bedrock (Quaide and Oberbeck, 1968), the regolith in the Fra Mauro region is estimated to range from 5 to 12 m in thickness (Eggleton and Offield, 1970). Material with a seismic (P wave) velocity of 104 m/s was measured to a depth of 8.5 m at the site of the *Active Seismic Experiment* (*ASE*) (Watkins and Kovach, 1972). This velocity is appropriate for unconsolidated material, and it is reasonable to assume that this represents the total regolith thickness at the ASE site.

TABLE 1.—*Numbers of craters counted in each area, numbers of craters calculated per 10^6 km^2, and crater ratios between Fra Mauro Formation and adjacent mare surfaces in outer ring of Sinus Aestuum*

[Wilhelms and McCauley, 1971]

Diameter (metres)	Cumulative number of craters counted: Fra Mauro Formation, A (fig. 5), IV 120H3 (8,172 km^2)	B (fig. 5), IV120H3 (356 km^2)	B (fig. 5), III 133M (356 km^2)	Mare, C and D (fig. 5), IV 120H3 (9,440 km^2)
64– 128			265	
128– 256			186	
256– 512			95	
512–1,000	1,006	45	37	829
1,000–2,000	199	8	7	67
2,000–4,000	30			12
4,000–8,000	2			
Cumulative number of craters calculated per 10^6 km^2				
512–1,000	151,409	148,877	123,596	96,475
1,000–2,000	28,274	22,472	19,663	8,683
2,000–4,000	3,917			1,588
Crater ratio, Fra Mauro:Mare				
512–1,000	1.58	1.54	1.28	
1,000–2,000	3.26	2.59	2.26	
2,000–4,000	2.47			

The variations in morphology of craters at the Apollo 14 site indicate a homologous series of craters of different ages. The age sequence of craters along the traverses from oldest to youngest is interpreted as follows (Eggleton and Offield, 1970) (pl. 1):

(1) Highly subdued craters expressed as very gentle depressions at the landing spot of the LM, west of the LM in the area of ALSEP deployment, and north of station A.

(2) The crater designated North Triplet, the moderately subdued 50-m crater east of station F, and the moderately subdued 10-m crater at station A.

(3) Cone crater and the sharp 45-m crater at station E.

(4) The sharp 30-m crater at station C′ and the small 10-m crater next to which a football-size rock was collected during the first EVA.

GEOLOGY OF THE FRA MAURO SITE

The geology of the site is divided into (1) the surficial geology or, more specifically, the character of the regolith, and morphologic features in, or reflected through, the regolith; and (2) the bedrock geology or, more specifically, the lithologic characteristics of local Fra Mauro Formation beneath the regolith. Because no exposures of bedrock were found during the mission, the nature of the Fra Mauro Formation must be inferred from rocks in the regolith that appear to have been derived from the underlying bedrock.

The geologic map (pl. 1) is derived from the study of photographs taken from lunar orbit and from the lunar surface. The map units therefore are based primarily on the morphologic characteristics of the surface and do not necessarily correspond directly to lithologic or structural units within bedrock.

SURFICIAL FEATURES

Lunar surface characteristics near Cone crater, such as grain-size distribution and surface morphology, are markedly different from those at stations more than a crater diameter away (pl. 5, 7). The distribution of rocks more than 1 m in diameter in the traverse area, and the distribution of rocks more than 20 cm in diameter at the panorama stations, are shown on plate 7. The LM landing point and station A are in areas where rock fragments larger than 2 or 3 cm in diameter are sparse (fig. 9A). Stations B, F, and G are in areas where rock fragments up to 20 cm in diameter are relatively common (fig. 9B), and stations B2, B3, and C′ are in areas where rock fragments more than 20 cm in diameter are abundant (figs. 9C, D). Station H has a moderate number of rock fragments more than 20 cm in diameter. Rock fragments up to large boulder size are fairly common east of station B1 and become increasingly abundant from east of station B1 to B2 to C′. The continuous ejecta blanket from Cone crater extends from the rim crest west to between stations B2 and B3 and is probably only patchy in the vicinity of station B1 (pl. 1; fig. 10). Farther west across the landing site, Cone crater ejecta occur only as isolated patches or along rays.

Surface material is noticeably finer grained at the LM and at stations A, B, B1, B2, F, G, and H than at stations B3 and C′ (see pl. 7). The topography where the surface material is finer is broadly undulating at wavelengths from tens to hundreds of metres and heights up to approximately 10 m. This topography characterizes old eroded craters, mostly of Eratosthenian and early Copernican ages. The topography at stations B3 and C′ is undulating at wavelengths from several metres up, and heights up to a metre or two. The undulatory surface topography in the vicinity of stations B3 and C′ reflects the original hummocky ejecta deposits from Cone crater.

The term regolith as used here refers generally to the debris layer that overlies the consolidated rock material of the lunar subsurface. The term can also be applied to a deposit that is developed on fragmental material such as the ejecta blanket of Cone crater; where it is used in this sense, it is specified. As previously stated, estimates of the thickness of the regolith at the Fra Mauro site range from 5 to 12 m. Seismic

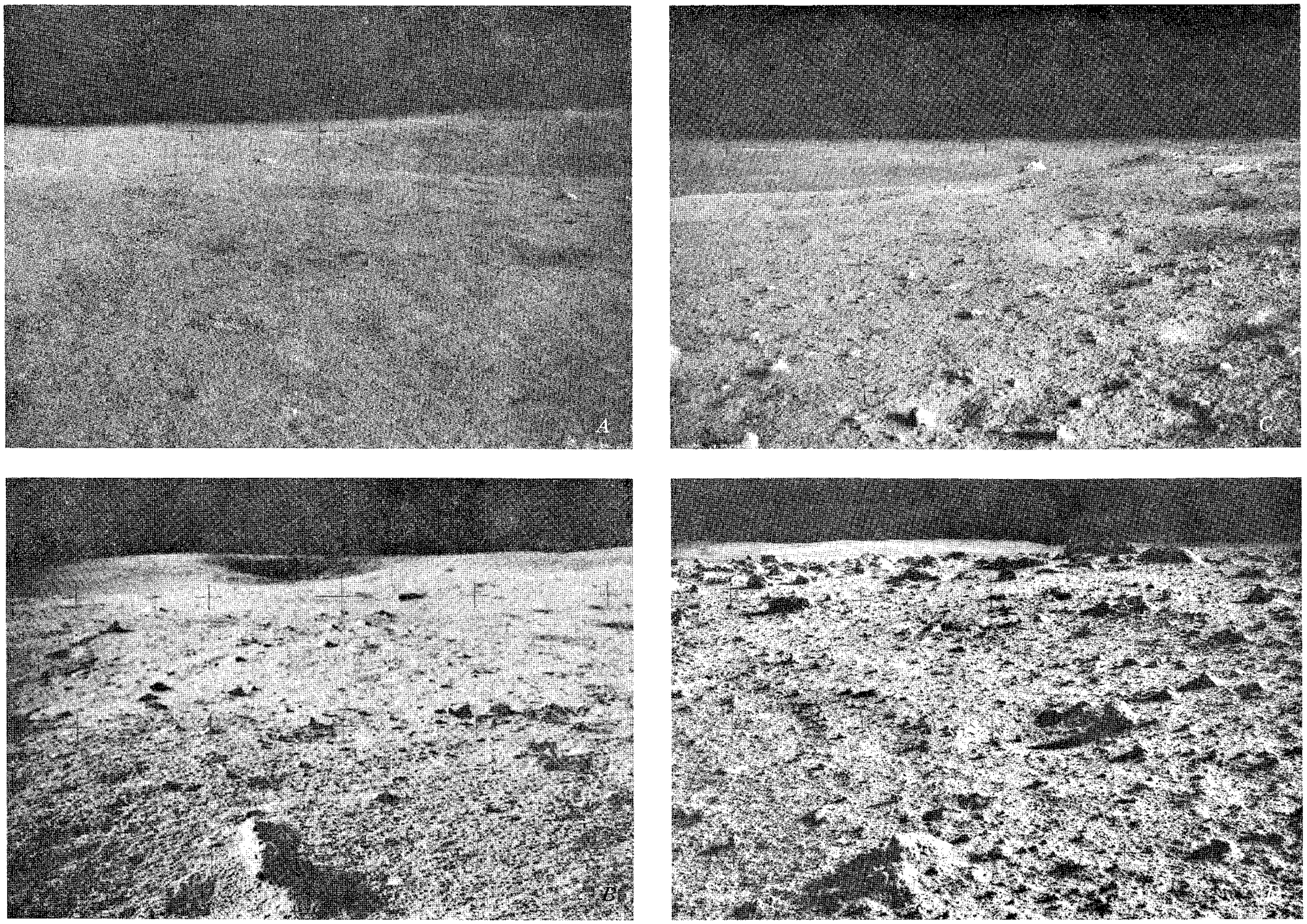

FIGURE 9.—Variation in abundance of rock fragments on surface in landing site area. *A*, View north from station A. Fragments in foreground are about 1 cm in diameter; boulder near center at middle ground is about ½ m in diameter. (NASA photograph AS14–68–9398.) *B*, View southeast from station F showing moderately abundant rock fragments. Old Nameless crater shows at horizon. Boulder in foreground is about 20 cm in diameter. (NASA photograph AS14–64–9152.) *C*, View north from station B3 showing abundance of rock fragments near the edge of the Cone crater ejecta blanket. The large boulder in the background is number 1005 on plate 6, pan 10. Fragments in foreground are 5–10 cm in diameter. (NASA photograph AS14–68–9432.) *D*, View northeast from the vicinity of station C′ showing abundance of rock fragments near Cone crater rim. Most fragments in foreground are 2–5 cm in diameter. (NASA photograph AS14–64–9106.)

data indicate a thickness of 8.5 m in the vicinity of the LM.

A rather continuous subdued ledge 9.5 m below the rim is visible in surface photographs of Old Nameless crater[2] located about 2.2 km south of station B2 (fig. 11). Below this ledge the walls of the crater are blocky. Just west of the rim crest of Old Nameless crater a small crater penetrates to slightly below the depth of the ledge and has blocky ejecta. This ledge is interpreted as the uppermost bedrock and suggests that the regolith is about 9.5 m thick in the vicinity of Old Nameless crater[3]. The actual thickness of the regolith in the Apollo 14 site probably varies because of the slopes of the ridges. In general, the regolith is probably somewhat thicker in the valleys and thinner on the ridge slopes and crests, largely because the trajectories of small crater ejecta are longer in the downslope direction than in the upslope (Soderblom, 1970).

[2]"Old Nameless" is the name applied to this crater by the crew of Apollo 13 for use in their landmark tracking during descent to the lunar surface. Apollo 13 did not land on the Moon owing to a spacecraft malfunction, and so the Apollo 14 mission was targeted for the Apollo 13 site. Apollo 14 was launched during a different time of year, so the ground track was not the same as that of Apollo 13, and Old Nameless crater was not used for a landmark. It therefore was not named on the Apollo 14 landing charts. The crew referred to it as Old Nameless, however, as they viewed it during the EVA's.

[3]A detailed study of Old Nameless crater on an AP/C analytical plotter showed that other features in the crater wall that appear as benches and possible layers are in reality the effect of light that is reflected from the upper surfaces of random hummocks.

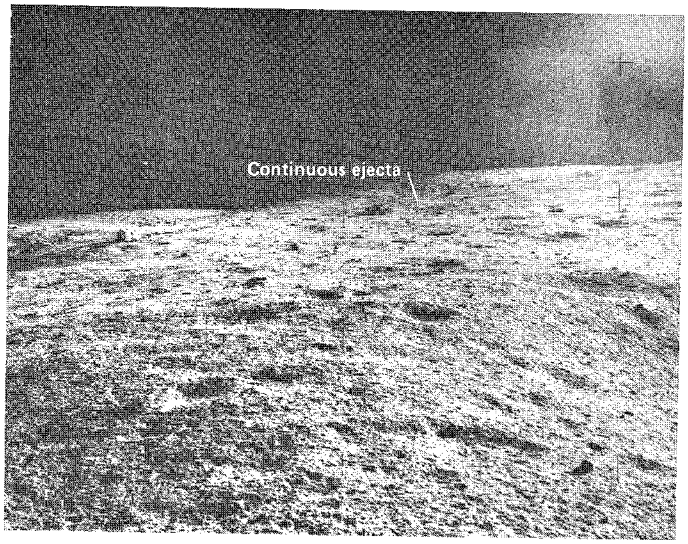

FIGURE 10.—View northeast from station B1 toward contact of Cone crater continuous ejecta about 175 m away. (NASA photograph AS14-64-9084.)

Although the rocks of the Apollo 14 and 16 sites are about the same age (Tatsumoto and others, 1972; Nyquist and others, 1972; Papanastassiou and Wasserberg, 1972; Kirsten, Horn, and Kiko, 1973), the regolith appears significantly thicker at the Apollo 16 site (fig. 12). The regolith is thick over old large craters which have been filled by erosion of their rims, and larger variations in regolith thickness are to be expected in the older areas of the Moon. During their early history, these areas were subjected to a high meteorite flux rate (Shoemaker, 1971, 1972), so that large craters were likelier to form. The regolith at the Apollo 17 site also appears to be thicker than at other sites. This could be explained by the presence of a large crater that has been destroyed by erosion, or by an addition of unconsolidated material such as volcanic ash and cinder, as was suggested by pre-Apollo 17 mapping (Scott and others, 1972).

The rate of regolith formation at the Apollo 14 and 16 sites, given a constant meteorite flux rate, should be somewhat higher than at the 11, 12, and 15 sites because the Apollo 14 and 16 breccias are somewhat more friable than are the basalts of the mare sites (fig. 13). However, the greater meteorite flux rate before flooding of the maria (Shoemaker, 1971, 1972) probably had a greater influence on this rate than did the difference in durability of materials.

The regolith that has developed on the Cone crater ejecta blanket appears to be thin. Small craters on the blanket have very blocky ejecta (fig. 14), which indicates that the ejecta of Cone crater has a higher internal abundance of rock fragments than is apparent at the surface and that overturning of the ejecta blanket by meteorite impact resulting in comminution of rocks has not extended to a significant depth. (See also sec-

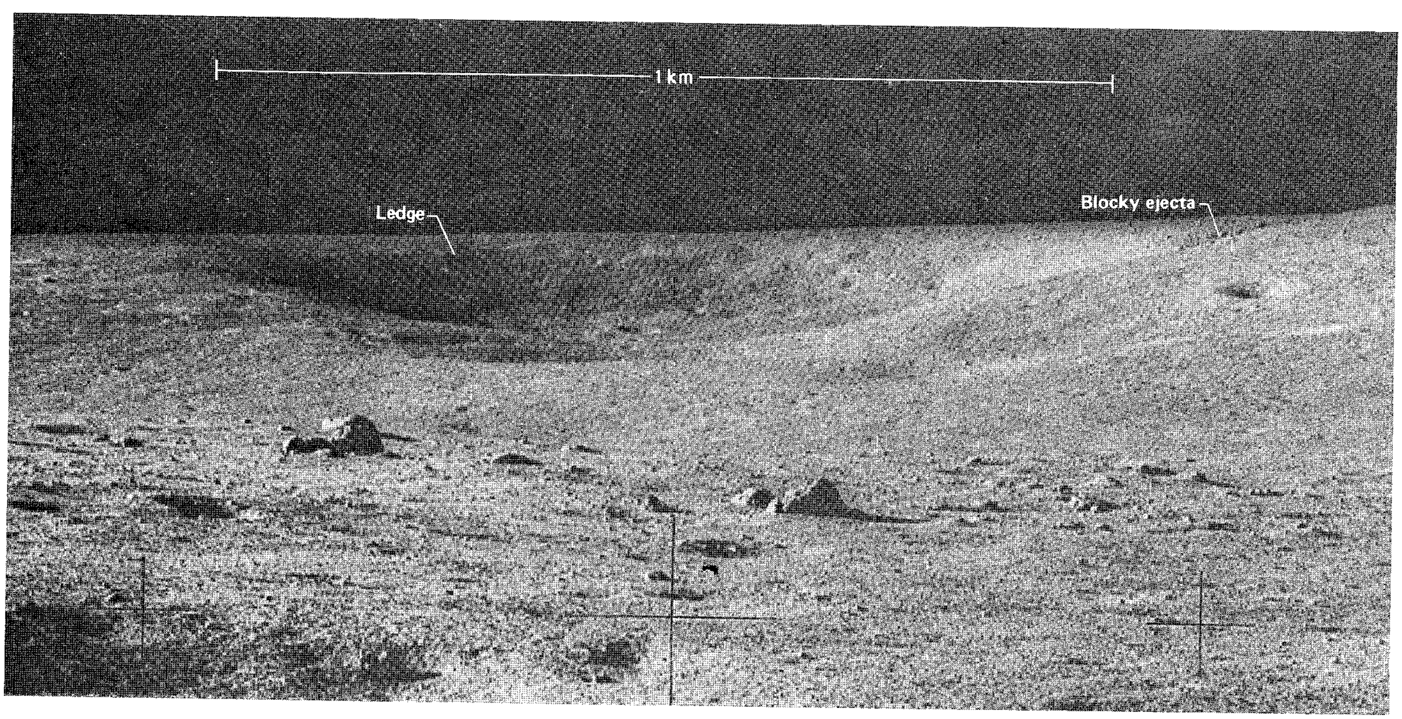

FIGURE 11.—Old Nameless crater, showing subdued ledge and blocky ejecta. View southeast from station B2. (Part of NASA photograph AS14-68-9425.)

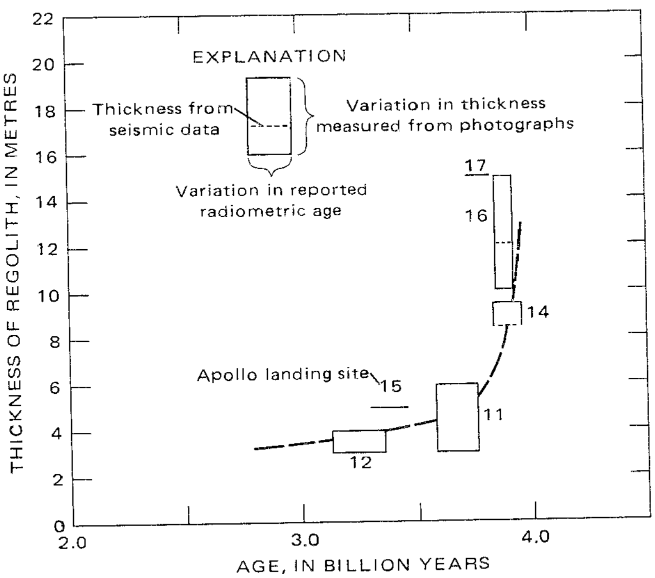

FIGURE 12.—Thickness of local regolith versus age of original surface as determined from radiometric ages of crystallization at Apollo landing sites 11–17.

tion entitled distribution of rock fragments.) The regolith on the Cone crater ejecta blanket is an immature, thin, and partial covering of fine-grained materials, some of which are probably original Cone crater ejecta, and some of which are products of erosion of rocks in the ejecta.

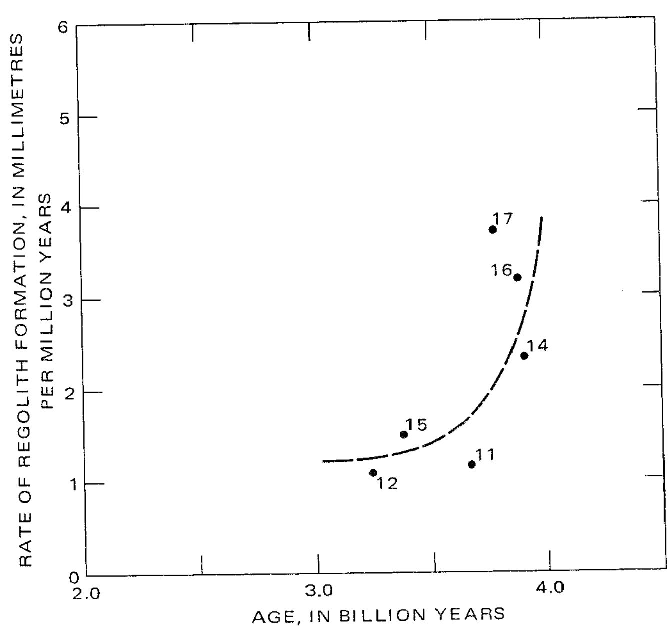

FIGURE 13.—Rate of regolith formation versus age of original surface as determined from radiometric ages of crystallization at Apollo landing sites 11, 12, 14–17. The values shown are median ages, and thicknesses from each landing site (numbered). The dashed curve was fitted by visual inspection.

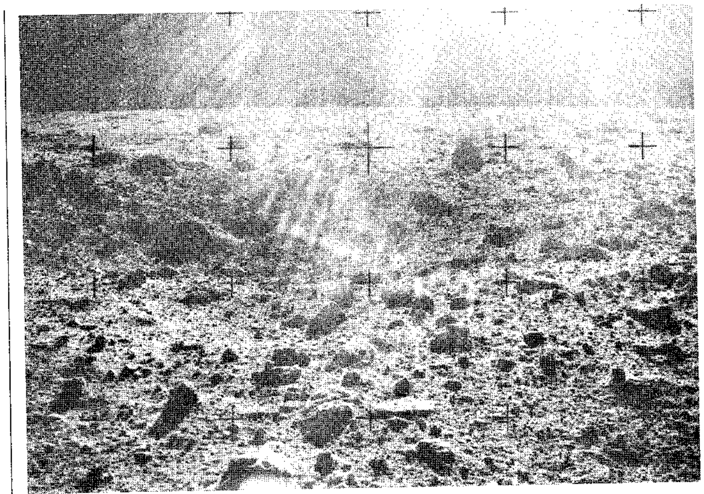

FIGURE 14.—Small crater in ejecta from Cone crater, with abundant blocks inside and on the rim of the crater. Fragments in foreground are 2–20 cm size. View east from station C′. NASA photograph AS14–64–9110.)

The smooth unit (Ifs, pl. 1) appears in Lunar Orbiter photographs to be a gently rolling terrane with a highly cratered surface. The ejecta blanket of Cone crater, however, is more hummocky and ridgy. These two types of surface morphologies extend down to centimetre scales. In order to evaluate the microrelief of the surfaces, detailed topographic maps with 1-cm contour intervals were constructed from two sample areas. Figure 15, an area west of the LM where sample 14304 was collected, shows that this surface is dominated by more or less equidimensional closed depressions. A similar map (fig. 16) at station C′, where a double core tube was driven, shows, in addition to the considerably higher abundance of rocks, that the surface is more hummocky and ridgy with a more complicated surface texture than that in the area west of the LM. Furthermore, at the location west of the LM, there are 27 craters between 10 and 50 cm in diameter in an 8 m^2 area; in the same location at station C′, there are only 6. It can therefore be concluded that a young surface created by ejecta from an impact crater tends to be ridgy and, as it grows older, tends to become one of coalescing closed depressions.

The Apollo 14 crew briefly described a "*raindrop pattern*" in the vicinity of station A similar to that previously described by the Apollo 12 crew. This pattern is readily seen in all of the panoramas, except at stations B3 and C′ (pl. 5), and in many of the sample documentation photographs (see figs. 50, 64, 66). It shows up best in photographs taken at low sun angle during EVA I (fig. 17). On fine-grained material the pattern appears to be formed by small craterlets up to 4 cm in diameter that saturate the surface. The raindrop pattern is interpreted to be formed by impact of small

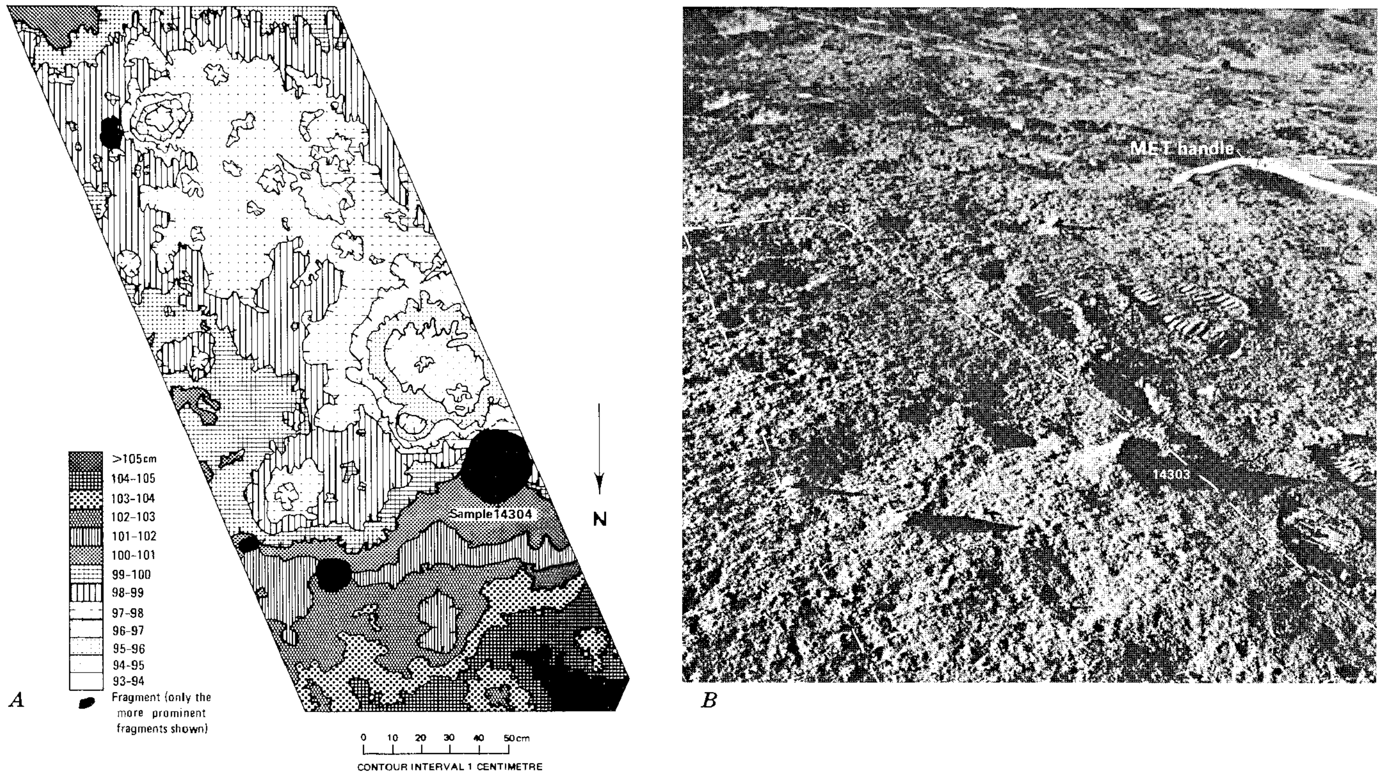

FIGURE 15.—Surface morphology west of the LM. *A*, Hypsographic map of surface in the vicinity of sample 14304, which was collected northwest of the LM. *B*, Photograph showing the map area. (NASA photograph AS14–67–9391.) Map prepared by Raymond Jordan.

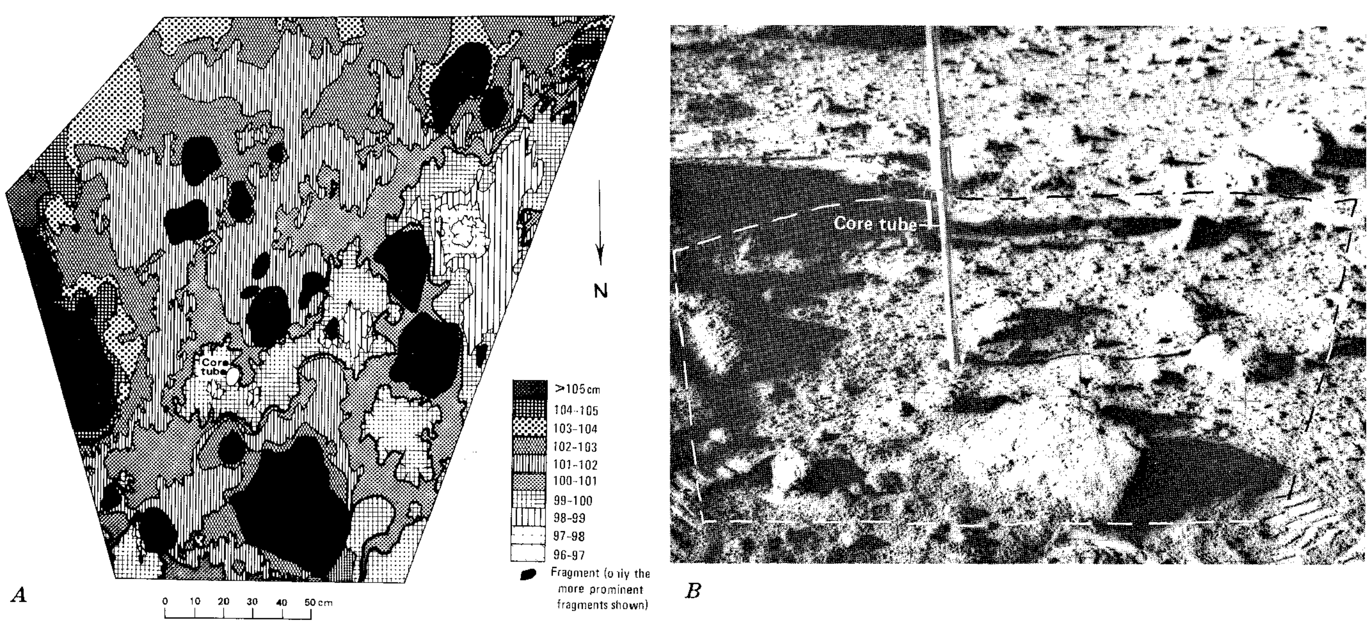

FIGURE 16.—Surface morphology near Cone crater. *A*, Hypsographic map of area where double core tube was driven at station C′. *B*, Photograph showing the map area. (NASA photograph AS14–64–9125.) Map prepared by Raymond Jordan.

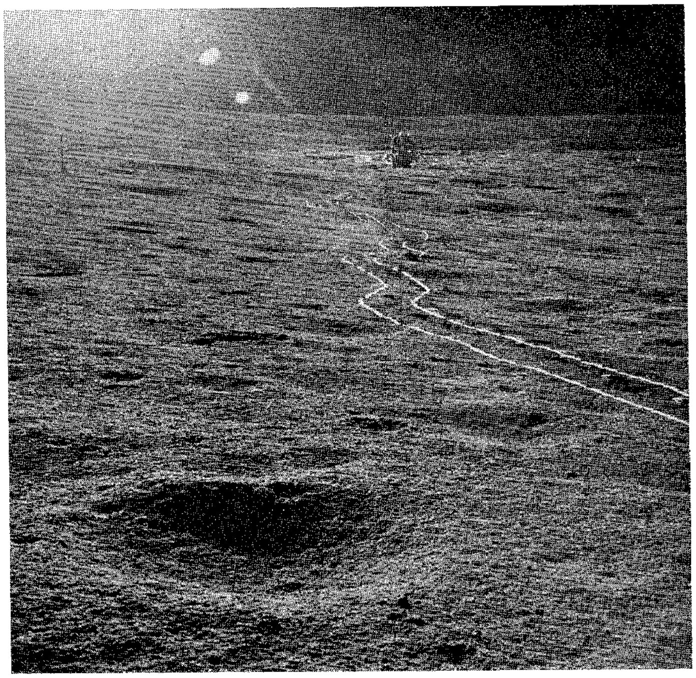

FIGURE 17.—"Raindrop" depressions on the surface of the smooth unit (pl. 1, unit Ifs) west of the LM. Bright lines are reflective tracks where the MET tires compressed the fine-grained material. View east. (NASA photograph AS14–67–9367.)

meteorites and by secondary particles from these impacts like those that form *"zap pits"* on rocks. A raindrop craterlet 1 cm deep is estimated to be destroyed by subsequent impacts in about 3 million years (Shoemaker and others, 1970), so that a fresh surface should become saturated by 4-cm craterlets in this time span.

Exposure ages of materials from Cone crater ejecta indicate that the crater was formed about 25–30 m.y. ago (Turner and others, 1971; Berdot and others, 1972; Crozaz and others, 1972). Where lighting is at a low incident angle to surfaces of boulders in Cone crater ejecta, zap pits are seen to cover the rock surfaces. This indicates that the surface of Cone crater ejecta should also be covered by a raindrop pattern, yet the pattern is much less evident in the ejecta blanket than in the western part of the area. Downslope movement of material, which would tend to destroy the craterlets, appears to have occurred on the steeper slopes on which the ejecta blanket was laid. Furthermore, the formation of craterlets would be impeded by the coarseness of the debris on the ejecta blanket. Small hummocks of fine-grained material a few centimetres in wavelength and height tend to obscure the craterlets. Also the sun angle was higher when the crew was on the ejecta blanket than it was during the first EVA, so the craterlets probably appeared less conspicuous.

DISTRIBUTION OF ROCK FRAGMENTS

Differences in the abundance of resolvable rock fragments at different stations along the traverse route are readily apparent on the panoramic photographs. It is also obvious that rock fragments are more abundant in the vicinity of Cone crater than elsewhere in the landing area. In order to help define the pattern and limits of Cone crater ejecta, boulders greater than 1 m across were plotted on the map of the landing site, and rock fragments more than 10 cm across were plotted on large-scale maps at each panorama station along the EVA II traverse route (pl. 7).

The areal distribution in the landing site of boulders more than 1 m across (approximate limit of resolution) was determined from Lunar Orbiter III photograph frame H–133. The densities of the boulder distributions were contoured at intervals of 1–2, 3–5, 6–10, 11–15, 16–20, and 21–25 boulders per 1,000 m^2, and the contours transferred to the rectified shaded-relief base. The lighting in much of the interior of Cone crater degrades the resolution, so that the densities shown in the regions of the map where the contours are dashed are probably lower than the actual densities. No boulders are visible in the totally shadowed region of Cone crater interior. Illumination of the remainder of the landing site favors identification of boulders, and therefore the counts are reasonably accurate.

Two bouldery ray patterns radiate from Cone crater, one to the north, and one to the southwest along the traverse area (pl. 7). Because the traverse route was along an identifiable ray, most if not all of the boulders along the traverse route, and probably many of the smaller fragments that were collected, are ejecta from Cone crater.

The area northeast of Cone crater is almost devoid of boulders, and so is the crater rim in this area. The variations in boulder abundances are probably due to differences in the physical characteristics of the Fra Mauro target materials before the Cone crater impact.

Much of the irregularity in ejecta patterns is probably the result of lithologic variations and fractures in the bedrock target materials of Cone crater. These must have been present from pre-Cone crater events, such as those that formed the Eratosthenian craters adjacent to Cone crater (pl. 1). A lens of friable material in the lower northeast part of Cone crater (pl. 1, geologic cross section) could explain the absence of boulders on the northeast rim.

In order to study areal distribution patterns of fragments too small to resolve on Lunar Orbiter photographs, fragments more than 10 cm across were plotted for 10 traverse stations on large-scale planimetric maps made from panoramic photographs taken with the Hasselblad cameras (pl. 7). The map areas are circles with 10-m radii; beyond 10 m, fragments up to 10 cm across are not accurately resolvable. The fragments are plotted to scale. The map distances and fragment sizes were determined from a perspective grid overlain on the panoramic photographs.

The maps show a general tendency toward an increase in the number of fragments greater than 10 cm toward Cone crater, which suggests an increase in the amount of Cone crater ejecta. The fragment population is slightly larger at station H than at the LM site and station A, which suggests an association of smaller fragments with the large rocks of station H (pl. 7).

The fragments within each map area are distributed somewhat nonuniformly. The fragment population is slightly larger in the southwest part of the station C′ map. Fragments are more abundant on the ejecta blanket of the small crater at C′ from which Cone crater ejecta was reexcavated than on the relatively undisturbed Cone crater ejecta (pl. 7).

Micrometeorite impact is generally considered to be the major cause of erosion on the lunar surface. (See for example Shoemaker and others, 1970.) Thus, on surfaces of similar materials, rock fragments larger than some minimal size should be less abundant on old surfaces than on younger surfaces, owing to longer exposure to erosion. The Apollo 14 site offers an excellent opportunity to test this hypothesis, in that surfaces of easily recognizable relative age differences along the traverse route were photographed in detail.

The surfaces in the traverse area are assigned relative ages on the basis of crater shapes and superposition (Eggleton and Offield, 1970). The ages of the surfaces of the areas in the station vicinities, from oldest to youngest, are: (1) station A in the relatively undisturbed Fra Mauro smooth unit; (2) station G approximately one-half crater diameter out on the ejecta of North Triplet crater; (3) stations B2 and C′ (looking northwest) on Cone crater ejecta; and (4) station C′ (looking southeast) on the ejecta of the 30-m crater at station C′.

In order to test the hypothesis that larger rock fragments are less abundant on older surfaces, the cumulative size-frequency distribution of resolvable rock fragments was determined for stations A, G, B2, and C′. Fragments 0.5 to 4 mm in size were counted on the *Apollo Lunar-Surface Closeup Camera* (*ALSCC*) photographs, fragments 4 mm to 1.6 cm in size were counted on the sample documentation photographs taken with the Hasselblad cameras, and fragments 1 m and larger were counted on the Lunar Orbiter photographs. No ALSCC photographs were taken at stations B2, C′, or G, so photographic information on fine particles at these stations is not available. Areas for which the counts were made or shown on plate 7, along with the cumulative size-frequencies of fragments, plotted on $\log_2 \times \log_{10}$ graphs. The approximation of the data points along straight lines, which have Pearson r correlations of $-.96$ to $-.99$ on the log-log plots, indicates that the fitted lines are statistically valid.

The cumulative size-frequency distribution curves show a decrease in the number of fragments larger than 1 cm with increasing age of the surfaces. The variations in the slopes of the size-frequency distribution curves are related to the ages of the surfaces; the older the surface, the greater the slope of the curve. Station B2 is an exception in that much of its surface is about the same age as that of the Cone crater ejecta at station C′. It is, however, more than a crater diameter away from Cone crater. Coarse particles were originally not as abundant at this distance from the impact point as they were near the crater rim. Also it is beyond the thin edge of the continuous ejecta blanket (pl. 1), so that the pre-Cone crater surface is partly exposed in the area. A problem arises in that no means have been devised with which to confidently distinguish in Hasselblad and ALSCC photographs small clods of regolith that are produced by impact from small coherent rock fragments. At the Apollo 14 site many of the small rock fragments are indurated matrix materials of the Fra Mauro rocks; thus, in photographs they resemble weakly indurated regolith breccias. No clods of boulder size can be identified in the photographs; all boulders that can be studied in detail appear to be well-indurated breccias. A total of five slightly coherent breccia samples were collected from stations A, B, and C′. Particles of agglutinates caused by shock lithification of fine regolith material by meteorite impact are common in the soil samples (McKay and others, 1972). Therefore, many of the small fragments that were counted were probably not eroded from larger rocks but are instead, small clods of local regolith indurated by impact processes. However, if even half of the smaller particles that were counted are soil breccias, the deviation from the curves shown would not be significant on this type of logarithmic plot.

A composite of the individual curves (fig. 18) shows that they converge at about 6×10^5 to 1×10^6 particles per 1,000 m^2 at a particle size of about 5 mm. The convergence point of the curves for fragments on surfaces of markedly different morphologic maturities suggests a steady-state size of particles smaller than about 5 mm, with the rate of production of 5 mm and smaller soil breccia particles approximately equalling the rate of destruction of 5 mm and smaller particles by erosion.

The increase in the slopes of the curves with increase in the age of the surface as shown in figure 18 indicates that small particles are formed by erosion of larger

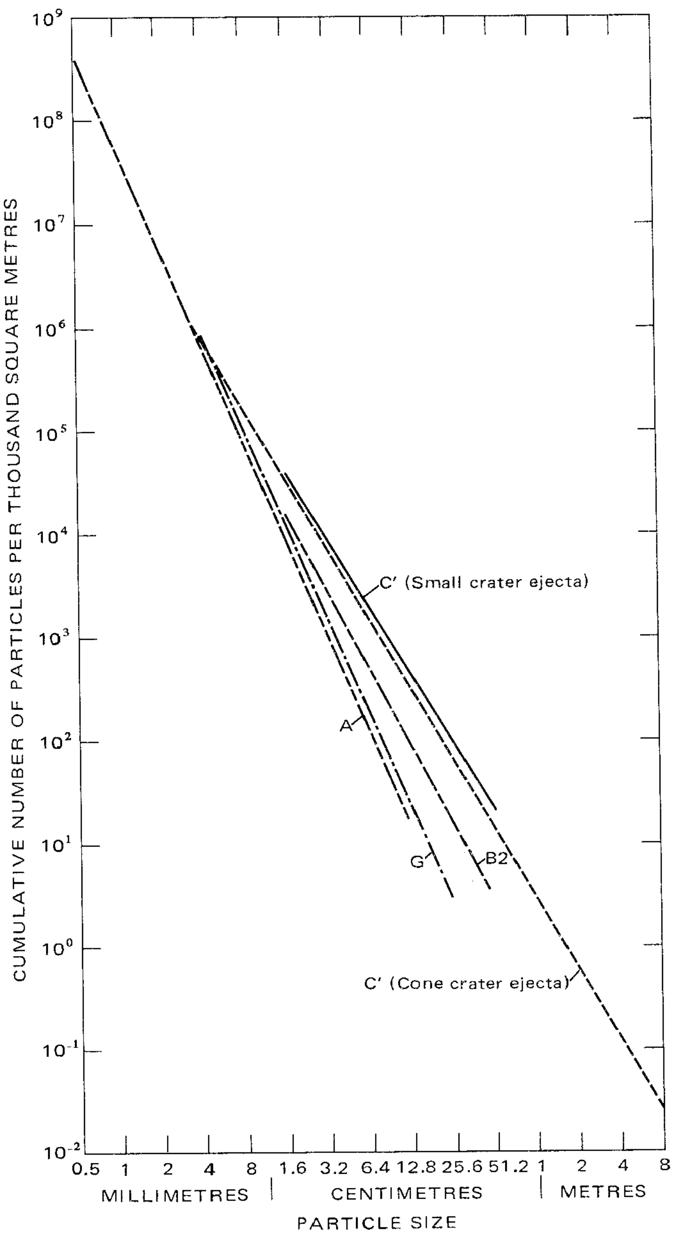

FIGURE 18.—Composite of fitted (least squares) size frequency curves for particles from 0.5 mm to 8 m. The curves and areas are shown individually on the graphs on the margins of the map on plate 7.

particles, and that, as the younger surfaces mature with time, the slopes of the curves will approach, and eventually exceed, that of the curve for station A by rotating around the convergence point. If no cratering events occur that are sufficiently large to excavate rocks from depth, a stage should be reached where the largest fragments are about 5 mm across, and all of these will be soil breccias. Continued stirring of the upper part of the regolith by small meteorites would both destroy and produce soil breccia particles that are about 5 mm across and smaller, and would continue to erode the remaining rock fragments, all of which would be smaller than 5 mm across. It is probable, however, that none of the lunar surface has been subjected to bombardment by small meteorites long enough for this stage of maturity to be reached, because occasional meteorite impacts with sufficient energy to excavate bedrock keep rejuvenating the rock fragment population on the surface.

FILLETS

Fillets have been defined as embankments of fine-grained material partly or entirely surrounding larger rock fragments (Shoemaker and others, 1968), and as accumulations of fine-grained material on uphill faces of rocks (Gault and others, 1967). They can be classified on the basis of shape into three groups: (1) concave, (2) low angle, and (3) convex (fig. 19). The shapes appear to be controlled largely by the attitude of the rock surface relative to the ground surface. Concave fillets are the most common and occur where the rock surface is steep. Low-angle fillets occur where the rock surface is also at a low angle and are generally shallow over the rock surface. Convex fillets are partly shielded by rock overhang and with time should develop into one of the other two types as the overhang volume is filled. The type that develops will depend on the shape of the rock surface above the overhang.

Mathematical models of fillet formation (Hait and Shoemaker, oral commun.) show that the common type concave fillet can be created from simple rebound of low-velocity, fine-grained particles striking the rock surface. The source for the fine particles is ejecta derived from small-scale impacts into the nearby regolith surface. The computer modeling simulated hemisphere (half-buried sphere), in a target area, on which particles were permitted to impact at varying incident angles and velocities. The preliminary results indicate that material eroding from the rock itself by spalling or micrometeorite erosion is not significant in fillet buildup, and that fillets are produced primarily by trapping of low-velocity materials ejected by cratering processes. A few rock fragments, however, are commonly seen on the fillet surface, and some are probably spalled from the rock.

This fillet model suggests that fillets grow with time and that their height might indicate the relative length of time that a rock has been in its present position on the lunar surface. However, variations in the heights of fillets on different boulders and smaller rocks that almost certainly were ejected from Cone crater, and thus have been at the surface for the same length of time, indicate that this is probably only a very qualitative indication of how long the rock has